University of Groningen

Spitzer's Mid-Infrared View on an Outer-Galaxy Infrared Dark Cloud Candidate toward NGC 7538

Frieswijk, W. F.; Spaans, M.; Shipman, R. F.; Teyssier, D.; Carey, S. J.; Tielens, A. G. G. M.

IMPORTANT NOTE: You are advised to consult the publisher's version (publisher's PDF) if you wish to cite from it. Please check the document version below.

Document Version
Publisher's PDF, also known as Version of record

Publication date:
2008

Link to publication in University of Groningen/UMCG research database

SPITZER'S MID-INFRARED VIEW ON AN OUTER-GALAXY INFRARED DARK CLOUD CANDIDATE TOWARD NGC 7538

W. F. FRIESWIJK,[1,2] M. SPAANS,[1] R. F. SHIPMAN,[2] D. TEYSSIER,[3] S. J. CAREY,[4] AND A. G. G. M. TIELENS[5]

ABSTRACT

Infrared dark clouds (IRDCs) represent the earliest observed stages of clustered star formation, characterized by large column densities of cold and dense molecular material observed in silhouette against a bright background of mid-IR emission. Up to now, IRDCs were predominantly known toward the inner Galaxy where background infrared emission levels are high. We present *Spitzer* observations with the Infrared Array Camera toward object G111.80+0.58 (G111) in the outer Galactic plane, located at a distance of ~3 kpc from us and ~10 kpc from the Galactic center. Earlier results show that G111 is a massive, cold molecular clump very similar to IRDCs. The mid-IR *Spitzer* observations unambiguously detect object G111 in absorption. We have identified for the first time an IRDC in the outer Galaxy, which confirms the suggestion that cluster-forming clumps are present throughout the Galactic plane. However, against a low mid-IR background such as the outer Galaxy it takes some effort to find them.

Subject headings: dust, extinction — infrared: ISM — ISM: clouds — stars: formation

1. INTRODUCTION

Massive stars are believed to form almost exclusively in stellar clusters (Blaauw 1964; de Wit et al. 2005), where supposedly the majority of all stars in the Galaxy form. The precursors to these stellar clusters are cold, dense, and most importantly, massive molecular clumps. A major, unexpected, and exciting result from the *Midcourse Space Experiment* (*MSX*) and *Infrared Space Observatory* (*ISO*) is the discovery of dark clouds seen in silhouette against the bright mid-IR background toward the inner Galactic plane (Egan et al. 1998; Perault et al. 1996). In contrast to the well-known dark clouds seen in visual extinction against the stellar distribution, these so-called infrared dark clouds (IRDCs) have much higher column densities ($\gtrsim 10^{23}$ cm^{-2}), are at large distances ($\gtrsim 1$ kpc), and hence are typically much more massive. Follow-up studies (e.g., Carey et al. 1998; Teyssier et al. 2002; Simon et al. 2006b) show that they are cold (<20 K), dense (~10^5 cm^{-3}), and indeed, among the most massive molecular clumps yet found in our Galaxy ($M \sim 100$–10^5 $M_\odot$). Many IRDCs contain compact (sub-) millimeter cores ($M \sim 10$–10^3 $M_\odot$, $n \sim 10^3$–10^7 cm^{-3}, $T \sim 15$–30 K; e.g., Carey et al. 2000; Teyssier et al. 2002; Garay et al. 2004; Rathborne et al. 2006). While these cores were first considered to represent the prestellar core phase of clustered star formation, recent studies show that at least some cores in IRDCs contain protostellar objects (e.g., Redman et al. 2003; Ormel et al. 2005; Rathborne et al. 2005). Nevertheless, IRDCs are likely to represent the earliest stages of clustered star formation (e.g., Menten et al. 2005; Rathborne et al. 2006), and they are generally referred to as cluster-forming clumps. Their ambient physical conditions can illuminate the role of IRDCs in the star-forming process and can provide insight into the differences between low- and high-mass star formation, the nature of the initial mass function, and the impact of environment on star formation. Moreover, their core-forming properties may reveal the important mechanisms involved in forming high-mass stars, e.g., competitive accretion, merging of lower mass stars, or massive disk accretion (e.g., Larson 2007 and references therein).

The identification of IRDCs is by necessity biased toward cold molecular clouds having sufficient column density against a bright mid-IR background, in order to be seen as absorption features. Hence, identifying IRDCs is considerably easier toward the mid-IR bright spiral arms and molecular ring in the inner Galactic plane (Simon et al. 2006a), i.e., within 90° from the Galactic center. An unbiased, more complete understanding of clustered star formation and its dependence on environment and other external properties, e.g., interstellar radiation field, metallicity, external pressure, and dynamics, requires a study of IRDC-like objects in more quiescent regions, such as the outer Galaxy, i.e., between $l = 90°$ and $l = 270°$.

W. F. Frieswijk et al. (2008, in preparation) produce a catalog of extended red objects in the outer Galactic plane. The objects are identified in the Two Micron All Sky Survey Point Source Catalog (2MASS ; Skrutskie et al. 2006) as clusters of stars that show a statistically redder color distribution compared to their local surroundings. A sample, consisting of 414 objects covered by the Canadian Galactic Plane Survey (CGPS; Heyer et al. 1998), was investigated in detail using the CO data of the CGPS. Over 90% of the objects correlate morphologically with CO emission with a typical FWHM of the order of 5 km s^{-1}. This suggests that the observed reddening is due to the presence of foreground molecular clouds. The kinematic distance of the clouds, derived from the CO radial velocity, indicates that ~15% are located beyond ~3 kpc from us. Some of these distant clouds (~10) do not show significant mid- and far-IR emission in, e.g., *MSX* and *IRAS*, and are potentially cold, cluster-forming clumps in the outer Galaxy, or "IRDC-like" objects. Frieswijk et al. (2007, hereafter F07) studied the physical characteristics of a candidate IRDC-like object (G111) by using molecular line observations. At a radial velocity of -52 km s^{-1}, G111 is located at a kinematic distance of ~5 kpc, assuming IAU standard constants. However, within 15′

[1] Kapteyn Astronomical Institute, P.O. Box 800, 9700 AV Groningen, Netherlands; frieswyk@astro.rug.nl, spaans@astro.rug.nl.
[2] National Institute for Space Research, P.O. Box 800, 9700 AV Groningen, Netherlands; R.F.Shipman@sron.nl.
[3] ESAC, Urb. Villafranca del Castillo, P.O. Box 50727, Madrid 28080, Spain; David.Teyssier@sciops.esa.int.
[4] *Spitzer* Science Center, California Institute of Technology, MC 314-6, 1200 East California Boulevard, Pasadena, CA 91125; carey@ipac.caltech.edu.
[5] NASA Ames Research Center, MS 245-3, Moffett Field, CA 9435-1000; Alexander.G.Tielens@nasa.gov.
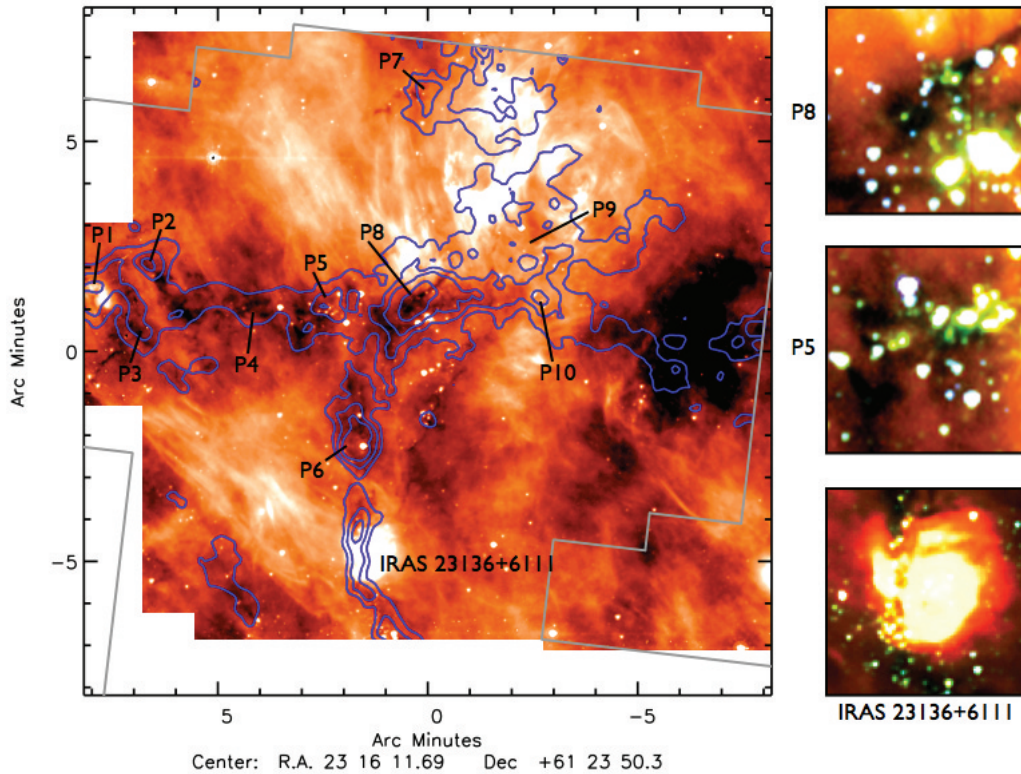
Fig. 1.—IRAC 8 μm emission toward the dark cloud complex G111. The contours depict the integrated C^{18}O (2–1) emission between -56 and -46 km s^{-1}, corresponding from outside in to 2, 3, 4, and 6 K km s^{-1} (adopted from F07). The gray line outlines the area covered by the C^{18}O observations. The P-numbers represent target positions from F07. The right images show a false-color close-up of positions P8, P5, and IRAS 23136+6111. The displayed emission is from the four IRAC channels, i.e., 3.6 μm (*blue*), 4.5 μm (*green*), 5.8 μm (*yellow*), and 8 μm (*red*).

on the sky and at similar radial velocity are the (massive) star forming regions NGC 7538 and S159. These are part of the Cas OB2 complex in the Perseus spiral arm, located at ~3 kpc from us and ~10 kpc from the Galactic center. Hence, a distance of 3 kpc is assumed for G111. A detailed investigation of the molecular lines conducted by F07 revealed multiple cold and massive cores (P1–P10; see Fig. 1 and § 4) along a filamentary cloud structure. The main conclusion is that G111 has global properties in agreement with values found for IRDCs, e.g., $M \gtrsim 3000 \, M_{\odot}$, $N \gtrsim 10^{23}$ cm^{-2}, $T \lesssim 20$ K. The mass and density of individual cores are low when compared to submillimeter cores in IRDCs. However, with peak column densities in excess of 10^{23} cm^{-2}, the most massive cores in G111 should, provided that sufficient mid-IR background is present, be observable as absorption features in a similar way to inner-Galaxy IRDC cores.

We subsequently requested *Spitzer* observations toward G111 to test the idea that the cores can be observed in absorption. *MSX* observations were not able to resolve this, presumably because the low sensitivity did not allow a detection of contrast between the molecular cloud and the background. With the sensitivity of the Infrared Array Camera (IRAC) on *Spitzer* we argued that it should be possible to observe this contrast. In this Letter, we present the first outcomes of the data. Combined with the results in F07, we conclude that we have, beyond doubt, a detection of an IRDC in the outer Galaxy. The Letter is organized as follows: § 2 gives an overview of the observations. Section 3 presents the results. In § 4 we discuss the observations and give our interpretation of the data

compared to the results published in F07. We conclude the section with some future prospects.

2. OBSERVATIONS

The data presented in this Letter are part of a larger project that focuses on the star formation characteristics of cluster-forming clumps in the outer Galaxy. The 3.5–8 μm observations were carried out on 2007 October 23 using the IRAC instrument on the *Spitzer Space Telescope*. Additional IRAC data are expected, as well as 24 μm data from the Multiband Imaging Photometer (MIPS) on *Spitzer*. These will be used to analyze the protostellar content of the region. However, the emphasis of this Letter is to present the first identification of an IRDC in the outer Galaxy. For that purpose, the present data are adequate.

The IRAC observations consist of a cycling 7-point dither pattern with medium-scale step size in high dynamic range mode. The data were processed and transformed into mosaic images using the data processing pipeline version S16.1.0 provided by the *Spitzer* Science Center. An integration time of 10.4 s per pointing resulted in an rms noise at 8 μm of ~0.05 MJy sr^{-1} and a point-source sensitivity of ~10 μJy. Additional calibration of the data is certainly required for the analysis of band-merged images. However, the standard pipeline produces data of sufficient quality to examine the contrast at 8 μm presented in this Letter.

3. RESULTS

Figure 1 shows the 8 μm emission toward G111. The image reveals a dark, filamentary structure against a bright and diffuse mid-IR background. The diffuse emission resembles the feathery cirrus emission first observed with the *Infrared Astronomical Satellite* (*IRAS*; e.g., Low et al. 1984). The cirrus observed with *IRAS* is assumed to be predominantly local, but here at least part of the emission appears to be located behind G111 ($\gtrsim 3$ kpc).

The contours show the integrated $C^{18}O$ (2–1) emission observed by F07. The dark structures match the contours of the $C^{18}O$ strikingly well. This implies that we observe a cold, dense molecular cloud, unlike the dark "hole" appearing at the right side of the image, where we do not see a match with $C^{18}O$. The locations in the figure indicated by the numbers P1–P10 represent target positions observed in detail by F07. The positions were selected on basis of their high column density. The physical properties derived by F07 suggest that they represent cold and dense molecular cores where stars might form. We briefly summarize their properties and relate these with the current observations in § 4.

The 8 μm image reveals several clusters of pointlike objects along the cloud filaments, most noticeably near P5 and P8. The upper two panels on the right of Figure 1 display false-color close-ups of these positions in the four IRAC bands, i.e., 3.6 μm (*blue*), 4.5 μm (*green*), 5.8 μm (*yellow*), and 8 μm (*red*). The lower panel displays a close-up of the bright source IRAS 23136+6111. The intensities there are scaled so that the dark lane, corresponding to the $C^{18}O$ filament, stands out clearly against the emission of the *IRAS* source.

We quantify the correlation between the dark features observed in the *Spitzer* data and the integrated $C^{18}O$ intensity by determining the mean 8 μm diffuse emission in increasing $C^{18}O$ emission bins. In order to remove the contribution of bright point sources, we first smooth the 8 μm image with a median filter of 11 pixels wide (1 pixel = 1.2″). We choose a $C^{18}O$ bin size of 1 K km s^{-1} and use only the region that is actually covered by the $C^{18}O$ observations. The results are given schematically in Figure 2. The first bin in the diagram represents an estimate of the background, determined from several positions in the image away from the dark cloud, after filtering as described above. An alternative background estimate is provided by the second bin in the diagram, which represents the 8 μm diffuse emission at any position where the $C^{18}O$ emission is less than 1 K km s^{-1}. The last bin of the diagram represents the lowest 8 μm emission toward locations where there is $C^{18}O$ emission in excess of 1 K km s^{-1}. The dashed boxes for each bin represent the scatter of the 8 μm emission. Note that the scatter is significant in the lower $C^{18}O$ bins (1–4 K km s^{-1}) because the extended, bright 8 μm emission falls within these contours (see Fig. 1).

If we adopt a background emission of 21 MJy sr^{-1}, and assume that the low emission, i.e., 13 MJy sr^{-1}, is purely due to absorption by the molecular cloud, then we can estimate the extinction. Using standard conversions given in the IRAC data handbook, the decrease in 8 μm emission of 8 MJy sr^{-1} corresponds to 0.5 mag of extinction. This value represents only a lower limit. Both the cloud and the background are contaminated by emission from foreground material and zodiacal light. The contribution of the zodiacal light is 4.2 MJy sr^{-1}, adopted from the *Spitzer* observation planning tool (SPOT). The foreground is difficult to determine. If we conservatively (remember the cloud is at 3 kpc) assume a foreground emission con-

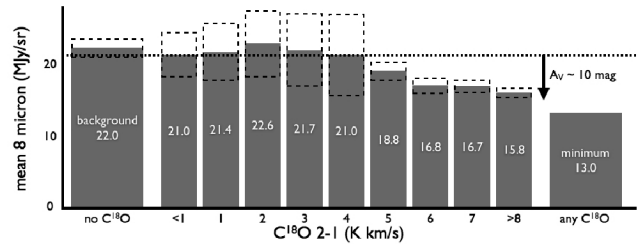FIG. 2.—Schematic view of the correlation between $C^{18}O$ (2–1) and the 8 μm diffuse emission. The dotted line represents a background of 21 MJy sr^{-1}. Even though the scatter, indicated by the dashed boxes, is significant for low $C^{18}O$ emission, the trend is clear. The brighter $C^{18}O$ emission, i.e., higher column densities, corresponds to the lowest mid-IR emission.

tribution of 4 MJy sr^{-1}, then the magnitude of the extinction at 8 μm is unity. For convenience, the mid-IR extinction can be expressed in terms of visual extinction using $A_V \sim 25 \times A_{8\mu m}$, where a standard conversion is adopted from Rieke & Lebofsky (1985). The arrow in Figure 2 corresponds to an A_V of 10 mag assuming a background of 21 MJy sr^{-1}.

4. CONCLUSIONS

The mid-IR properties of G111 compare well to other IRDCs. The *MSX* survey data have been used by Simon et al. (2006a) to identify a large number of IRDCs in the inner Galaxy by their mid-IR contrast relative to the background. A typical 8 μm extinction observed toward IRDCs, determined from the ratio between the on- and off-source emission after foreground and zodiacal light correction, is 1–2 mag (e.g., Egan et al. 1998; Carey et al. 2000). We find extinction values toward G111 to be in agreement with this, at least toward the darkest cores. More so, the extinction measurement gives only a strict lower limit to the column of material. The cloud does not only absorb background emission, but reradiates low-level emission as well. For a cold dark cloud (<25 K) this will be negligible. However, once embedded objects start heating parts of the cloud it may become important. The contrast between the cloud and the background, and thus the measured extinction, decreases as the cloud emits, but of course the column of material does not. The molecular column densities of positions P1–P10 are $\sim 10^{22}$ cm^{-2}, peaking at $\approx 7 \times 10^{22}$ cm^{-2} for P8 (F07). The latter corresponds to 2.8 mag extinction at 8 μm (70 mag in A_V).[6] These estimates demonstrate that parts of this cloud have a mid-IR extinction comparable to values found for inner-Galaxy IRDCs (e.g., Carey et al. 1998; Hennebelle et al. 2001).

Recall in this that the selection of IRDCs from *MSX* data is based on high contrast (Simon et al. 2006a). In the outer Galaxy, a high contrast is not guaranteed because of the low-level background emission. For example, compare the background of the IRDCs toward the edge of W51, i.e., ~60 MJy sr^{-1} (IRAC/MIPS cycle 1 observations; K. Kraemer et al. 2005, private communication) with the background that we observe (~20 MJy sr^{-1}). Note that one bright 8 μm emission feature clearly is in the background of G111, since a dark lane is visible in front of IRAS 23136+6111 (see Fig. 1, *lower close-up*).

The four-color images show a clustering of starlike objects near the dark filaments. Although these stars could coincidently be in the foreground, this positional consistency suggests that some cores might have started to form stars. The excess in stellar surface density was also pointed out by F07 toward P5

---

[6] This is a factor of 2 above the value in F07, because of a too low conversion factor used by F07.

and P8, based on the 2MASS data. Note that IRDCs are often associated with active star formation (e.g., Redman et al. 2003; Rathborne et al. 2005). Star-forming activity may further reveal itself by the presence of "green fuzzy emission," i.e., as weak extended 4.5 μm features. This emission is often attributed to shocked gas arising from outflow activity, e.g., the pure rotational H_2 lines $S(11)$ at 4.18 μm through $S(9)$ at 4.69 μm and the rovibrational lines of CO at 4.45–4.95 μm (e.g., Noriega-Crespo et al. 2004; Marston et al. 2004). Shocked-gas features are, besides for nearby star formation, also frequently observed toward IRDCs (e.g., Rathborne et al. 2005; Beuther & Steinacker 2007). A first impression of the emission at 4.5 μm suggests that such features are present toward some cores in G111. However, further investigation is required to confirm this.

4.1. *Notes on Individual Cores*

The positions P1–P10 in Figure 1 were selected by F07 based on their high column density. A detailed investigation showed that they represent cold (10–20 K), dense ($>10^3$ cm^{-3}), and massive cores (~100 $M_\odot$, P8 ~ 1000 $M_\odot$) where stars might form. Star-forming activity was investigated by means of 2MASS star colors and star counts and the presence of warm gas (NH_3, ^{13}CO). The following discussion summarizes some of the results in F07 and includes the mid-IR characteristics of the cores presented in this Letter.

P1, P2, P3, and P7 do not show indications of active star formation. P1 shows enhanced 8 μm emission, which may be a chance encounter along the line of sight. The other cores show a decrease in 8 μm emission, corresponding to an A_V of >10 mag. The peak extinction appears somewhat offset from the $C^{18}O$ peak, which is true for most cores. This may be explained by $C^{18}O$ freeze-out in the densest regions. P4 is not a core but part of the $C^{18}O$ filament extending to the east. Several extinction peaks at 8 μm ($A_V \gtrsim 10$ mag) are present. P9 and P10 are not evident as cores in $C^{18}O$ and show no specific features at 8 μm. P6 shows a decrease of 8 μm emission ($A_V \gtrsim 7$ mag), but the contrast with the background may be reduced due to the presence of the bright source near the $C^{18}O$ peak. Whether this source is physically associated cannot be determined at present. P5 and P8 show signs of active star formation. The NH_3 lines indicate the presence of warm gas. Both cores have associated 2MASS sources with typical near-

IR colors of YSOs. Furthermore, the stellar surface density of 2MASS peaks at a value almost twice that of the surrounding field for P8. These results are supported by the four-color images that reveal signs of active star formation in the form of clustering of objects and 4.5 μm "green fuzzes." The 8 μm contrast indicates peak extinctions of at least 12.5 mag in A_V for both cores. IRAS 23136+6111 was not a target position in F07, but is nonetheless interesting to include here. $C^{18}O$ emission reveals a narrow filamentary structure. The four-color image depicts a dark lane and a clustering of point sources matching the location of the filament. We thus conclude that it must be in the foreground of the bright *IRAS* object. Further investigation is required to see if the dark lane and the *IRAS* source are associated, which may indicate a triggered star-forming event.

To summarize, the *Spitzer* observations support the results in F07. Except for P5 and P8, where star formation may have started, the cores appear to be in a cold, prestellar phase.

4.2. *Future Prospects*

Supplemental IRAC and MIPS 24 μm data from *Spitzer* are expected. Combining the IRAC bands with the 2MASS data enables a discrimination between stars and YSOs for many of the clustered point sources in the cloud vicinity. Adding 24 μm data will allow a proper SED modeling of the dust emission. The characteristic features of envelopes, disks, and photospheres in the SED will enable a determination of the evolutionary state, i.e., Class 0, I, II, or III, of the apparent discrete sources (e.g., Robitaille et al. 2007). Star-forming activity can be further characterized through an analysis of the spatial distribution and strength of polycyclic aromatic hydrocarbon emission (e.g., 3.3, 6.2, and 7.7 μm covered by the 3.6, 5.8, and 8 μm bands, respectively) and shock activity, exemplified by the 4.5 μm features in the close-up images in Figure 1 (e.g., bow shocks; Neufeld et al. 2006; Velusamy et al. 2007). Considering the distance to the cloud, high-resolution continuum and spectroscopic observations (near-IR to millimeter) are essential to improve on the spatial information.

Facilities: Spitzer(IRAC)

REFERENCES

Beuther, H., & Steinacker, J. 2007, ApJ, 656, L85
Blaauw, A. 1964, ARA&A, 2, 213
Carey, S. J., et al. 1998, ApJ, 508, 721
———. 2000, ApJ, 543, L157
de Wit, W. J., Testi, L., Palla, F., & Zinnecker, H. 2005, A&A, 437, 247
Egan, M. P., Shipman, R. F., Price, S. D., Carey, S. J., Clark, F. O., & Cohen, M. 1998, ApJ, 494, L199
Frieswijk, W. W. F., et al. 2007, A&A, 475, 263
Garay, G., et al. 2004, ApJ, 610, 313
Hennebelle, P., et al. 2001, A&A, 365, 598
Heyer, M. H., et al. 1998, ApJS, 115, 241
Larson, R. B. 2007, preprint (astro-ph/0701733)
Low, F. J., et al. 1984, ApJ, 278, L19
Marston, A. P., et al. 2004, ApJS, 154, 333
Menten, K. M., Pillai, T., & Wyrowski, F. 2005, in IAU Symp. 227, Massive Star Birth: A Crossroads of Astrophysics, ed. R. Cesaroni et al. (Cambridge: Cambridge Univ. Press), 23

Neufeld, D. A., et al. 2006, ApJ, 649, 816
Noriega-Crespo, A., et al. 2004, ApJS, 154, 352
Ormel, C. W., Shipman, R. F., Ossenkopf, V., & Helmich, F. P. 2005, A&A, 439, 613
Perault, M., et al. 1996, A&A, 315, L165
Rathborne, J. M., et al. 2005, ApJ, 630, L181
———. 2006, ApJ, 641, 389
Redman, R. O., et al. 2003, ApJ, 586, 1127
Rieke, G. H., & Lebofsky, M. J. 1985, ApJ, 288, 618
Robitaille, T. P., Whitney, B. A., Indebetouw, R., & Wood, K. 2007, ApJS, 169, 328
Simon, R., et al. 2006a, ApJ, 639, 227
———. 2006b, ApJ, 653, 1325
Skrutskie, M. F., et al. 2006, AJ, 131, 1163
Teyssier, D., Hennebelle, P., & Pérault, M. 2002, A&A, 382, 624
Velusamy, T., Langer, W. D., & Marsh, K. A. 2007, ApJ, 668, L159